

**Biochemical and histopathological effects of Spinosad on males of red palm weevil *Rhynchophorus ferrugineus* (Olivier) (Coleoptera: Dryophthoridae)**

**Salaheldin Abdelsalam**

*Department of Zoology and Entomology, Faculty of Science, Assiut University, Egypt*

**Received:** 21/6/2016

**Accepted:** 3/8/2016

The red palm weevil, *Rhynchophorus ferrugineus*, is of great concern worldwide, especially in the Middle East, where dates are a strategic crop. Despite their ecological hazard, insecticides remain the most effective means of control. A bioinsecticide of bacterial origin, spinosad is effective against several pests, and its efficacy against male *R. ferrugineus* was assessed in the present study. The antioxidative responses of key enzymes including catalase (CAT), superoxide dismutase (SOD) and glutathione-S-transferase (GST) to spinosad were investigated in the midgut and testes. Moreover, the effects of this insecticide on the cell ultrastructure of the midgut, Malpighian tubules and testes were also determined. The LC50 of spinosad was measured at 58.8 ppm, and the insecticide inhibited the activities of CAT, SOD and GST in the midgut. However, no significant changes in the activities of these enzymes were observed in the testes. Spinosad treatment resulted in concentration-dependent changes in the cellular organelles of the midgut, Malpighian tubules and testes of *R. ferrugineus*, and some of these effects were similar to those exerted by other xenobiotics. However, specific changes were observed as a result of spinosad treatment, including an increase in the number and size of concretions in Malpighian tubule cells and the occasional absence of the central pair of microtubules in the axonemes of sperm tails. This study introduces spinosad for potential use as an insecticide within an integrated control program against male red palm weevils. Additionally, the study provides biochemical and ultrastructural evidence for use in the development of bioindicators.

**Keywords:** Spinosad; *Rhynchophorus ferrugineus*; midgut; Malpighian tubules; testis; antioxidants; ultrastructure

## **INTRODUCTION**

The red palm weevil, *Rhynchophorus ferrugineus* Olivier (Coleoptera: Dryophthoridae), is a fatal pest to coconuts and date palm trees. Currently, *R. ferrugineus* has spread to Oceania, throughout the East [1], and to Europe and the Americas [2]. Dates, an important crop in the Middle East, are strongly threatened by the red palm weevil, and several methods have been applied to control this pest, including plant quarantine treatments, improved farming practices, insecticides and pheromone traps. Insecticides are by far the most

efficient means of reducing weevil numbers, but these toxins cause environmental pollution and can damage other useful creatures. However, using biological control has proven effective against *R. ferrugineus* in the laboratory but not in the field [3], so the search for suitable and environmentally safe insecticides to combat the weevil continues. Spinosad is a low-risk insecticide of bacterial origin that balances the high effectiveness of insecticides against the environmental safety risks [4,5]. Spinosad has been used to control several pests, including coleopterans [6,7]. Spinosad attacks insects by activating a specific site at the nicotinic acetylcholine receptor and/or GABA receptor [8–10]; these spinosad target sites in both receptors differ from those of other neonicotinoid insecticides, such as imidacloprid [11].

Treating insects with insecticides often induces the production of reactive oxygen species (ROS), which may be the cause of death, but defensive enzymes enable insects to eliminate ROS [12,13]. Superoxide dismutase (SOD) converts superoxide radicals into oxygen and hydrogen peroxide [14], which in turn requires another enzyme, such as CAT, for its conversion into water and oxygen [15]. GST supports the defense against insecticides and plays a major role in the development of resistance [16]. The published data on the biochemical effects of spinosad on such defensive enzymes in insect cells are limited; therefore, the present study aimed to elucidate the effects of the insecticide on key defensive enzymes (e.g., SOD, CAT and GST) in the midgut and testes of male *R. ferrugineus* and on the ultrastructure of the midgut, Malpighian tubules and testes.

## MATERIALS AND METHODS

### Insect-rearing Technique

Red palm weevils were obtained from infested palm trees in Al-Ahsa Governorate in the eastern region of Saudi Arabia and were cultured in a rearing room at  $25 \pm 2^\circ\text{C}$ ,  $70 \pm 5\%$  RH, and a photoperiod of 12:12 h (L:D); the adults were fed apple slices. Adult sexing was determined according to the presence of a stripe of black hairs on the dorsal-frontal part of the male snout.

## Bioassay

Spinosad (PESTANAL®, analytical standard) was purchased from Sigma-Aldrich Laborchemikalien GmbH, Germany and dissolved in 70% ethanol; serial dilutions of 10, 50, 100, and 200 ppm were prepared using 10% sucrose. The solutions were supplied to the adult males in 0.5-ml Eppendorf tubes with pierced, flat caps, and the snout of each adult was inserted into the tube to allow them to feed on the spinosad solutions. The insect bodies were gently fixed to the feeding tubes using thin Parafilm strips, and each insect with its accompanying feeding tube was placed in a 100-ml plastic cup, which was covered with a perforated plastic cap. Four replicates of five insects each were tested at each insecticide concentration, and the mortality ratios were recorded after 24 h. Mortality was corrected according to Abbott [17]. The control treatment consisted of 10% sucrose for feeding. Pearson's correlation coefficient was used to check the association between insect mortality and spinosad concentrations.

## Biochemical Investigations

Treated and untreated males were dissected in cold 67 mM potassium phosphate buffer (pH 7), and the testes and midgut were removed and stored separately in 1.5-ml tubes at  $-80^{\circ}\text{C}$  until use. The frozen tissues were homogenized in the same buffer, and the resulting homogenates were centrifuged at  $10,000 \times g$  for 15 min at  $4^{\circ}\text{C}$ . The supernatants were removed into new tubes and used as enzyme sources. SOD activity was measured using nitroblue tetrazolium (NBT) as a substrate [18], and the diluted homogenate (0.5 ml) was mixed with 0.5 ml of 0.4 mM NBT in 50 mM potassium phosphate buffer (pH 7.8). The reaction was monitored by reading the absorbance at 490 nm, and SOD activity was calculated using an extinction coefficient of  $12.8 \text{ mM}^{-1} \text{ cm}^{-1}$ . The resulting values are expressed as units per min per mg protein. CAT activity was measured as described by Aebi [19]. The diluted tissue homogenate from each sample (0.5 ml) was added to 0.5 ml of 30 mM hydrogen peroxide, the loss of which was measured by reading the absorbance at 240 nm over 3 min at 30-sec intervals. CAT activity was calculated using an extinction coefficient of  $0.0436 \mu\text{M}^{-1} \text{ cm}^{-1}$  and is expressed as  $\mu\text{mol}$  of decomposed hydrogen peroxide per min per mg protein.

GST activity was measured according to Habig *et al.* [20]. Samples were prepared by mixing 100  $\mu\text{l}$  of homogenate with 10  $\mu\text{l}$  of 0.2 M 1-chloro-2,4-dinitrobenzene (CDNB) and 150  $\mu\text{l}$  of 10 mM reduced glutathione; the reaction was monitored by reading the absorbance at 20-sec intervals for 5 min at 340 nm. The activity was calculated using an extinction coefficient of  $0.0096 \mu\text{M}^{-1} \text{cm}^{-1}$  and is expressed as units per min per mg protein.

The total protein contents of all samples were estimated using a commercial kit (MicroLowry, Peterson's modification, Sigma). The data were analyzed using SPSS 17.0 for Windows (SPSS Inc., Chicago, IL) and are presented as the means  $\pm$  standard errors (SE). Statistical analysis consisted of one-way analyses of variance (ANOVA) followed by post-hoc tests and the level of significance were set at  $P < 0.05$ .

#### Electron Microscope Studies

Insect tissues were pre-fixed in 3% glutaraldehyde in phosphate buffer (pH 7.4) for transmission electron microscopy. After post-fixing in 1% phosphate-buffered osmium tetroxide, the specimens were dehydrated in an ethanol gradient and embedded in Araldite. Ultra-thin sections were cut using an ultramicrotome (EM UC7, Leica Ltd., Germany), stained with 2% uranyl acetate and lead citrate, and observed under a Jeol 1011 transmission electron microscope (Jeol Ltd., Japan) at 80 kV.

## RESULTS

The mortality ratio in the control treatment was 5%, indicating that the use of feeding tubes did not affect survival. All tested spinosad concentrations resulted in concentration-dependent mortality (Table 1), and the tested concentration and the number of dead individuals within each group was highly correlated ( $r = 0.94$ ;  $P < 0.05$ ). The LC<sub>50</sub> was calculated as 58.8 ppm.

Table 1. Mortality of male *R. ferrugineus* exposed to serial dilutions of spinosad

Spinosad concentration (ppm)	Number of exposed males	Number of dead males	Mortality (%)
0	20	1	5
10	20	3	15
50	20	11	55
100	20	13	65
200	20	18	90

SOD activity in the midgut of males that were fed with 10 ppm spinosad was significantly lower than that in the control group (Figure 1A). SOD activity in the midgut of males that were fed with 50 ppm spinosad was insignificantly higher than that observed in males fed with 10 ppm spinosad, and high spinosad concentrations (100 and 200 ppm). SOD activity changes in the testes in response to all treatments were insignificant compared with those in the control group (Figure 1B).

All spinosad concentrations effectively reduced CAT activity in the midgut (Figure 1C), and CAT activity in the testes was much higher than that in the gut (Figure 1D). However, CAT activity did not significantly change in the testes in response to the tested spinosad concentrations. GST activity in the midgut was significantly reduced by spinosad at all tested concentrations compared with the control group (Figure 1E), but no significant differences were found among the various concentrations. In the testes, no significant changes in GST activity were observed between the control group and all treatment groups (Figure 1F). Generally, CAT, GST activity levels were higher in the testes than in the midgut.

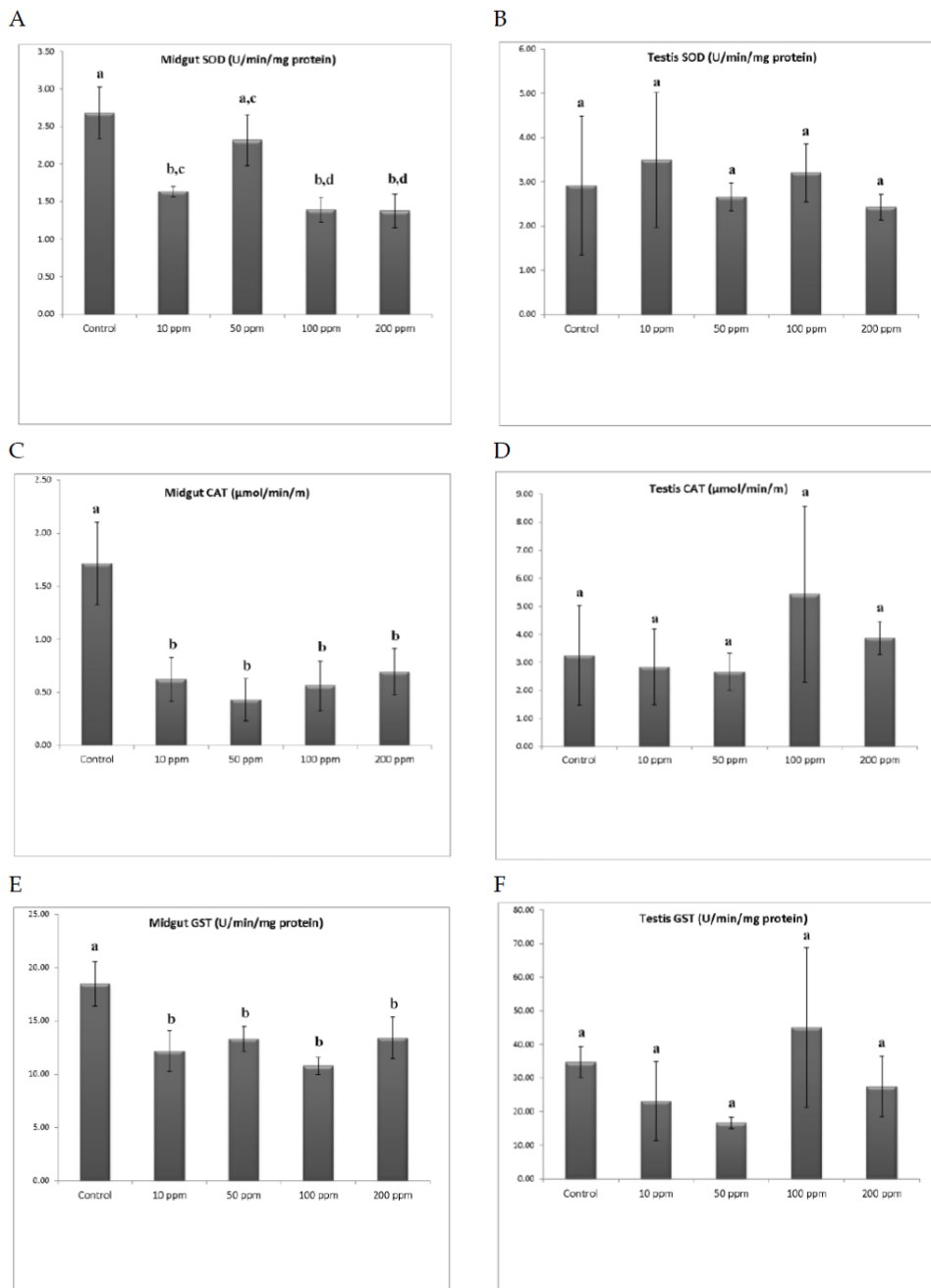


Fig 1. Antioxidant enzyme activities of control and spinosad-treated male *R. ferrugineus*. Each bar represents the mean  $\pm$  SE of three replicates. Bar superscripts, without a common letter differed significantly from each other; the level of significance was  $P < 0.05$ .

Electron Microscope Observations

The midgut epithelium of the control group was characterized by an apical striated border including numerous, long microvilli extending into the midgut lumen (Figure 2A). Abundant and dense mitochondria, parallel arrays of rough endoplasmic reticulum (RER) cisternae, ribosomes, few lysosomal bodies and an oval cell nucleus with fragmented heterochromatin were evident (Figure 2B). Glycogen and lipid inclusions were also visible in the cytoplasm, and the midgut cells were laterally joined by long septate junctions, which were tight and intact. Cytological observations of the spinosad-treated groups revealed a dramatic, concentration-dependent cytotoxicity of the midgut epithelial cells. The microvilli in weevils that were treated with 10 ppm spinosad were withered, detached and fragmented, or even partially lost. The nuclear chromatin became more concentrated into patches of varying densities, and many lysosomes, including heterolysosomes and autophagic vesicles, were scattered in the cytoplasm (Figure 2C). The mitochondria exhibited visible damage; their cristae were fractured and dissolved. The RER membranes were obviously reduced, destroyed and occasionally dilated; thus, their layer structure was lost (Figure 2D). Treatment with higher spinosad concentrations resulted in further cellular injury (Figure 2E). Cytoplasmic vacuolization also increased, and vacuoles united in some cases, forming large clear zones within the cells. Moreover, structural disruption of the septate junctions between the columnar cells was most common in insects treated with 100- and 200-ppm spinosad (Figure 2F, G). The junctional membranes were no longer continuously apposed to their adjacent counterparts, and the membranes appeared fully internalized into the cell cytoplasm in some cases (Figure 2H). There was also an increase in the number of inter- and intracellular spaces, and abundant clusters of lipid droplets were encountered in most of the damaged epithelia.

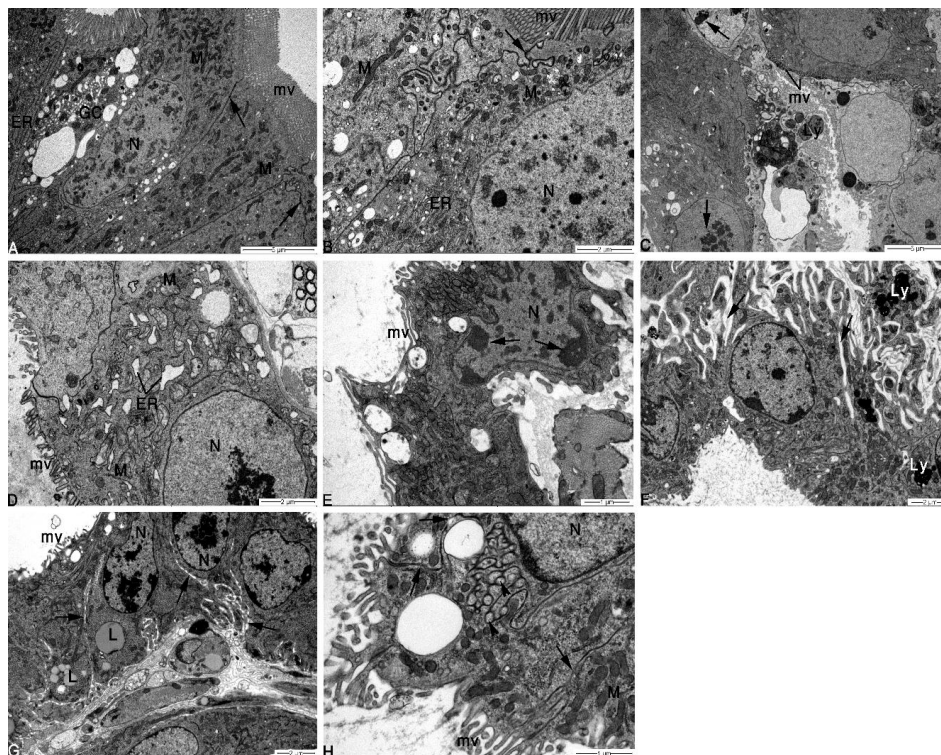
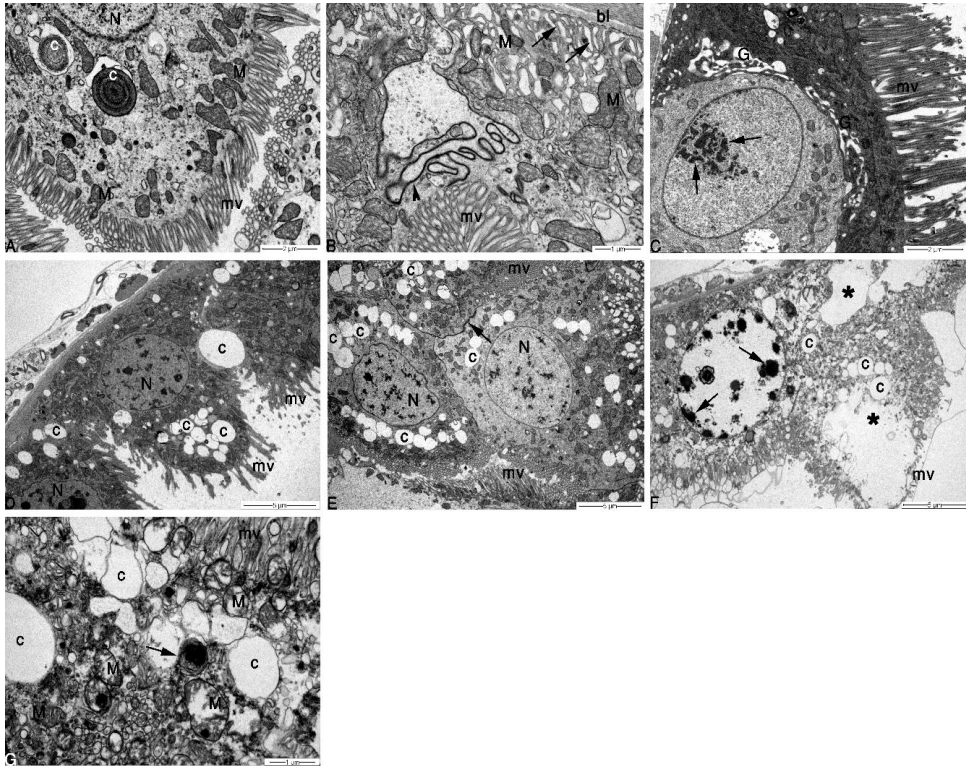


Figure 2. Transmission electron microscopy of *R. ferrugineus* midgut epithelial cells. Control (A, B): (A) Observe the closely spaced microvilli (mv), oval nucleus (N), abundant mitochondria (M), well-developed cisternae of the endoplasmic reticulum (ER), intact septate junctions (arrows), and Goblet cells (GC). (B) A high-magnification image of the apical region of control epithelial cells depicts tightly packed microvilli (mv), a nucleus with homogenous chromatin (N), electron-dense mitochondria (M), arrays of endoplasmic reticulum (ER), and a normal septate junction (arrow). Spinosad (10 ppm) (C, D): (C) Note the damage to the apical microvilli (mv), nuclei with chromatin at different condensation levels (arrows), and the increased amount of lysosomal bodies (Ly) passing into the gut lumen. (D) Mitochondria (M) appear swollen; the cristae are partially disintegrated, and the ER shows dilated cisternae. Fragmented microvilli (mv) can also be seen. (E) Spinosad (50 ppm): Corrugated and indented nuclei (N) with chromatin concentrated at the edge (arrows). The epithelial cells are no longer columnar, and the microvilli (mv) are severely disoriented. (F) Spinosad (100 ppm): Marked dilations of junctions (arrows) between epithelial cells. Microvilli are less

developed over part of the cell surface. Nucleus (at the lower left) is irregular and deformed, and large heterolysosomes (Ly) are discernible in the cytoplasm. Spinosad (200 ppm) (G, H): (G) Note condensed nuclei (N), extensive lipid accumulation (L) in the cytoplasm, and abnormal dilations of junctions between cells (arrows). Also, the microvilli (mv) and ER arrays are only scanty. (H) Septate cell junctions are disrupted with apparent gaps (arrows) and sign of internalization in the cytoplasm, arrowheads indicate dilated parts of septate junctions, mv: ruptured microvilli, N: nucleus, M: mitochondria with indistinct cristae.

The apical part of the Malpighian tubule cells of control *R. ferrugineus* had regular microvilli that were closely parallel to each other (Figure 3A). Frequently, the microvillar border contained finger-like extensions of the mitochondria, which were quite numerous in the cortical cytoplasm and between the infoldings of the underlying basement membrane (Figure 3B). Septate (tight) junctions were characteristic at the lateral margins of adjacent cells, and globules with concentric membrane rings (i.e., laminated concretions) were also found in the upper and central parts of cells that were closely associated with the Golgi bodies or endoplasmic reticulum. The nuclei were spherical or slightly elongated, and the chromatin was homogenous with a few heterochromatin granules clumped along the nuclear envelope. The nucleolus was well developed. Spinosad treatment caused concentration-dependent ultrastructural changes in the epithelium of the Malpighian tubules compared with the control. When the weevils were treated with spinosad at low concentration (10 ppm), the microvilli were regressed, and the nucleus had several patches of heterochromatin (Figure 3C). Similar degenerative changes were observed in insects treated with 50 and 100 ppm spinosad, but the concretions were larger and more closely packed, forming complex agglomerations (Figure 3D, E). Treatment with spinosad at 200 ppm resulted in large lytic areas within the cytoplasm (Figure 3F), and the mitochondria were swollen with altered cristae and electron-lucent matrices. Large numbers of small and large concretions were present, and lysosomes (myelin-like structures) accumulated within the cytoplasm. Some nuclei had irregular, indented shapes, and the chromatin exhibited abnormal clumping, which gave the nucleoplasm a much less electron-dense appearance (Figure 3G). In some parts, the microvilli and basal interdigitations (or labyrinths) were completely missing. Mitochondria were also less frequent in the cytoplasm of treated weevils compared with those in the controls. Alzahrani et al. [21] and Paoli et al.

[22] recently described the detailed ultrastructure of *R. ferrugineus* testes. The germ cells and spermiogenic stages of the control group showed normal mitochondria (nebenkern), endoplasmic reticula (ER), Golgi bodies and flagellar axonemes (Figure 4). However, all spinosad concentrations produced concentration-dependent defects in the developing spermatids and mature sperm. Exposure to 10 or 50 ppm spinosad produced minor alterations; Golgi bodies and mitochondria were clearly swollen, and ER membrane whorl development was extensive (Figure 5A, C, D). Sperm heads were mostly free of detectable abnormalities, except for a few cases of disturbed karyoplasm or binucleated sperm (Figure 5B). Exposure to 100 ppm spinosad also showed signs of mitochondrial swelling and degeneration. Some spermatids exhibited unrecognizable remnants of cell organelles due to advanced cellular injury and vacuolization; such cells also contained intracytoplasmic inclusions (debris), myelin-like membranes, and dense, osmiophilic granules of diverse sizes (Figure 5E). The most obvious morphologic abnormalities were seen in testes after treatment with 200 ppm spinosad. Some spermatogenic cells were totally eroded, and spermatogenesis appeared severely inhibited (data not shown). Many of the early spermatids were deformed and displayed abnormal chromatin compaction (karyopyknosis) (Figure 5F), possibly indicating cell death, which was accompanied by ER dilation and degranulation. The nuclear chromatin of later stages underwent insufficient condensation, showing distinct clear spaces and lacunae (i.e., immature chromatin), and their nuclear envelopes were remarkably irregular in outline (Figure 5G). In several cross-sectional profiles, the sperm tails appeared devoid of central axoneme microtubules (i.e., 9+9+0 pattern) (Figure 5H), and mitochondrial edema was distinctive. The mitochondrial matrices were distended and showed reduced stainability, and the cristae were mostly scarce or undeveloped (i.e., hypoplastic) (Figure 5I).



**Figure 3.** Transmission electron microscopy of Malpighian tubules of *R. ferrugineus*. Control (A, B): (A) Note the normal appearance of brush border microvilli (mv) containing mitochondria (M), and the laminated concretions (c) in the central cell cytoplasm, N: euchromatic nucleus. (B) The basal lamina (bl) has branched, irregular infoldings (arrows) forming a well-developed labyrinth associated with mitochondria (M), arrowhead points to convoluted septate junction, mv: microvilli. (C) Spinosad (10 ppm): Irregular microvilli (mv), nucleus with several patches of heterochromatin (arrows), and hypertrophied Golgi fields (G). (D) Spinosad (50 ppm): Irregularly arranged microvilli (mv), numerous concretions (c), N: nucleus with several dark clumps of chromatin. (E) Spinosad (100 ppm): Similar changes (as in D) but at a greater level. Arrow indicates septate junction. Spinosad (200 ppm) (F, G): (F) Lesions include large area of lysed cell cytoplasm (asterisk), chromatin clumping mainly at the nuclear periphery (arrows), enlarged laminated concretions (c), and destroyed microvilli (mv). (G) Abnormally large mitochondria (M) reveal prevalent existence of cristolysis and matrical loss (as compared to A). Note also myelin-like figure (arrow) with complex membrane whorls, large intracellular concretions (c), mv: deformed microvilli.

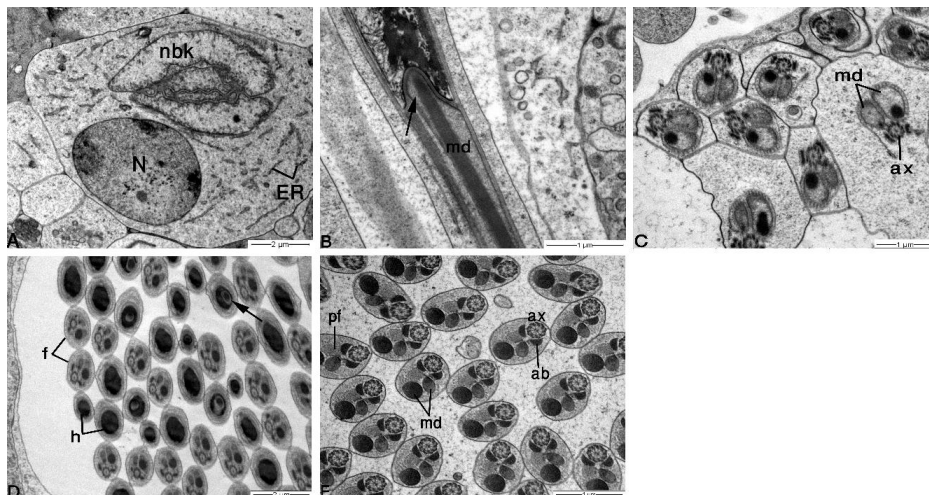


**Figure 4.** Transmission electron microscopy of normal spermiogenesis of control *R. ferrugineus*. (A) C.S. of early developing spermatids. (B) L.S. of late spermatid showing typical chromatin condensation. (C) C.S. of spermatid tails. (D) C.S. of sperm heads and flagella. (E) C.S. of sperm tails (magnified image). N: nucleus, ER: cisternae of endoplasmic reticulum, nbk: nebenkern, md: mitochondrial derivatives, arrow (in B and D) indicates extension of large md into infloding of the nucleus, ax: axoneme (9+9+2 arrangement of microtubules), h: head, f: flagellum, ab: accessory bodies, pf: puff-like structure.

## DISCUSSION

This research demonstrated that spinosad dissolved in 10% sucrose is toxic when ingested by male *R. ferrugineus*. Labelling the fluid level in the feeding tube before feeding provided a reliable way to ensure that the insect fed on the spinosad solution, and non-feeding males were excluded. A similar feeding apparatus was used to determine the gustatory response of boll weevils to spinosad [7]. The 24-h LC50 was measured as 58.8 ppm, and the LC50 of RADIANT (spinosad) when mixed with food was 18.7 ppm for the last instar of *R. ferrugineus* [23]. The 24-h LC50 of Tracer (24% spinosad) was 123.49 ppm for the third instar of *R. ferrugineus* [24]. The oral LD50 of spinosad, which causes acute toxicity in rats, is 3.738 mg/kg, and the dermal LD50 of spinosad in rabbits is 2,000 mg/kg. Therefore, the toxicity of spinosad toward farm animals or humans is minimal [25], and spinosad use is therefore a suitable adult-based feeding control technology for *R. ferrugineus*.

Insects usually respond to treatment with insecticides with increased antioxidation and detoxification enzyme activities to overcome the resulting ROS [26]. However, in the present study, all tested concentrations of spinosad significantly reduced the activity of SOD and CAT in the midgut. CAT knockdown of *R. ferrugineus* larvae results in significant growth inhibition and larval mortality [27]. Treatment with bioinsecticides, such as plant extracts [28] and hematoporphyrin photoinsecticides [29], resulted in SOD inhibition in cowpea storage beetle and flesh fly, respectively.

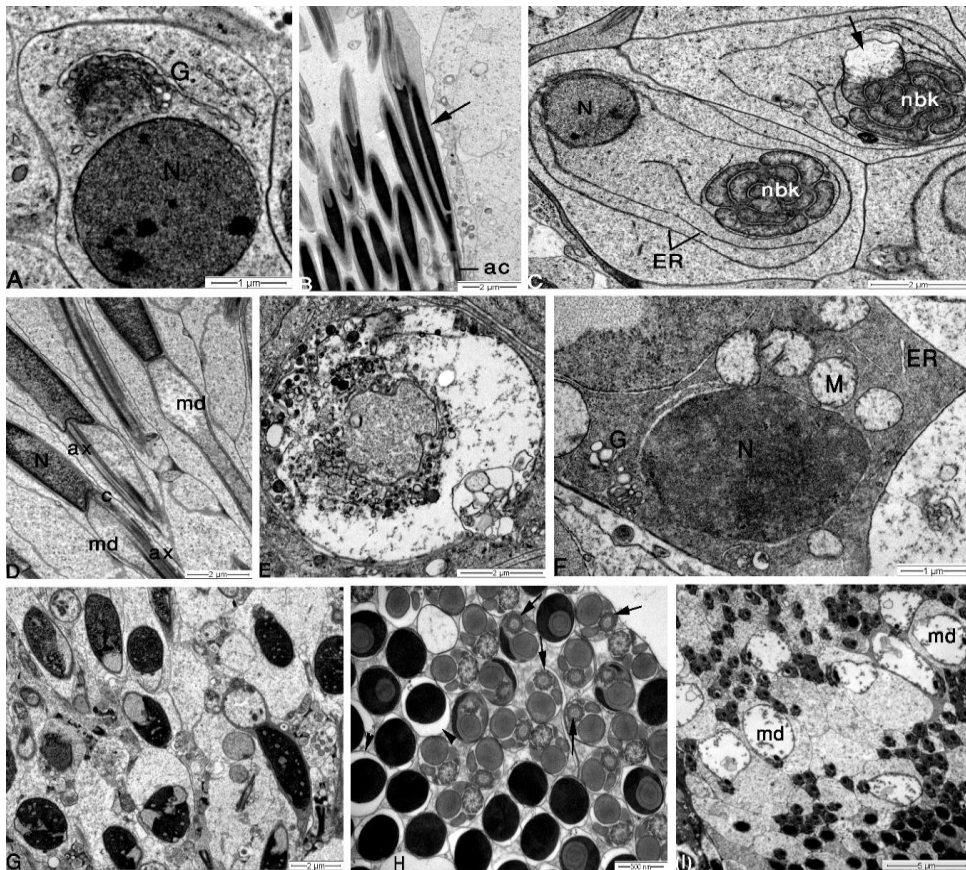


**Figure 5.** Transmission electron microscopy of testis of spinosad treated *R. ferrugineus*. Spinosad (10 ppm) (A, B): (A) C.S. of early spermatid showing hypertrophied Golgi body (G), N: nucleus. (B) L.S. of mature sperms. Arrow indicates binucleated sperm head, ac: acrosome. Spinosad (50 ppm) (C, D): (C) C.S. of early spermatids depicting ER-membrane whorls around nucleus

(N) and nebenkern (nbk). Arrow points to mitochondrial damage. (D) L.S. of late spermatids. Note extensive swelling of mitochondrial derivatives (md), N: nucleus, ax: spermatid axoneme, c: centriole. (E) Spinosad (100 ppm): C.S. of degenerating early spermatid. Spinosad (200 ppm) (F-I): (F) C.S. of early spermatid showing electron-dense nucleus (N), swollen mitochondria (M), dilated ER cistern, enlarged vesicles of Golgi body (G). (G) L.S. of late-stage spermatids. Note the abnormal chromatin coalescence. (H) C.S. of mature sperms. Axonemes lack central microtubules (arrows), and nuclear envelope of sperm is folded and dilated (arrowheads). (I) C.S. of sperm tails showing marked edematous changes in mitochondrial derivatives (md).

All spinosad concentrations used in the current study also inhibited GST activity in the midgut of *R. ferrugineus*. Conversely, spinosad treatment did not affect GST activity in the lepidopteran pests *Spodoptera exigua* or *Plutella xylostella* [30, 31] or in the beetle *Oryzaephilus surinamensis* [32]. Spinosad can be used synergistically with other insecticides that have been associated with insect resistant populations due to enhanced GST detoxification, such as pyrethroid and organophosphate-resistant pest populations [33]. Of note, no spinosad cross-resistance with other insecticides has been recognized [34]. Thus, spinosad is a good candidate for use in an integrated pest management program for *R. ferrugineus*. Resistance to spinosad has only been recorded with the involvement of a null mutation in the acetylcholine receptor subunit gene [35] or the activation of microsomal demethylase [30].

At all spinosad concentrations that were tested in this study, the activities of CAT, SOD and GST were not significantly altered in the testes of weevils. Therefore, other enzymes (such as P450 monooxygenases) may be involved in the detoxification of spinosad in the testes. A similar result was obtained with atrazine herbicide, which, although it resulted in histological changes in rat testes, did not affect CAT or SOD activity [36].

The results of the present study show that the epithelial cells of the midgut of *R. ferrugineus* males that were fed with spinosad showed signs of apoptosis, including condensed chromatin and vacuolization. Similar signs were observed in the midgut of *Spodoptera littoralis* larvae after treatment with spinosad [37] or other bioinsecticides [38]. In this study, signs of

phospholipidosis were clear, as represented by large heterolysosomes and myeloid bodies. Similarly, vacuolization and phospholipidosis were reported after spinosad treatment in mice [39].

Malpighian tubules are involved in insecticide detoxification because they host organic and inorganic anion transport processes [40]; therefore, the tubule epithelia might play a role in conferring bioinsecticide or chemical insecticide resistance. Intracellular concretion is characteristic of the principal cells of the Malpighian tubules, which are involved in salt secretion into the lumen of the tubules. In the present study, high concentrations of spinosad induced the overproduction of intracellular concretions, which indicates activation of the spontaneous transepithelial secretion of salts to dilute the secreted toxin [41]. Thus, Malpighian tubules may play a role in spinosad detoxification in *R. ferrugineus* males.

The ultrastructure of the testes of *R. ferrugineus* males that were treated with 200 ppm spinosad showed severe damage. The testicular damage can be viewed in the same context as that observed in the cellular organelles of the midgut and Malpighian tubules, and electron microscopy revealed an abnormal assembly of microtubules in sperm axonemes, which may cause motility defects [42]. Consistent with this finding, some carbamate insecticides have been shown to affect the *in vitro* polymerization of tubulin [43].

Taken together, these findings indicate that the cells of all studied tissues of spinosad-treated male *R. ferrugineus* showed similar organellar damage, including mitochondrial swelling, abnormal chromatin, and the destruction of membrane junctions. These common types of damage were observed in the brain and muscle cells of insects after treatment with fibronil [44]. Mitochondrial swelling indicates that spinosad targeted and disrupted mitochondrial energetics [45]; therefore, adenosine triphosphate (ATP) depletion is expected [46].

## CONCLUSION

This article reported the ultrastructural and biochemical effects of spinosad on *R. ferrugineus* tissues, and the findings may serve as ecotoxicological indicators for a deeper understanding of the spinosad mode of action.

## REFERENCES

1. Y. Li, Z. Zhu, R. Ju, L. and Sheng Wang, The red palm weevil, *Rhynchophorus ferrugineus* (Coleoptera: Curculionidae), newly reported from Zhejiang, China and update of geographical distribution. *Florida Entomol.*, 92, 386–387 (2009).
2. O. Dembilio, J. A. Jacas, Bio-ecology and integrated management of the red palm weevil, *Rhynchophorus ferrugineus* (Coleoptera: Curculionidae), in the region of Valencia (Spain). *Hell. Plant Prot. J.*, 5, 1–12 (2012).
3. G. Mazza, V. Francardi, S. Simoni, C. Benvenuti, R. Cervo, J. R. Faleiro, E. Llácer, S. Longo, R. Nannelli, E. Tarasco, P. F. Roversi, An overview on the natural enemies of *Rhynchophorus* palm weevils, with focus on *R. ferrugineus*. *Biol. Control*, 77, 83–92 (2014).
4. G. D. Thompson, K. H. Michel, R. C. Yao, J. S. Mynderse, C. T. Mosburg, T. V. Worden, E. H. Chio, T. C. Sparks, S. H. Hutchins, The discovery of *Saccharopolyspora spinosa* and a new class of insect. *Down to Earth*, 52, 1–5 (1997).
5. C. B. Cleveland, M. A. Mayes, S. A. Cryer, An ecological risk assessment for spinosad use on cotton. *Pest Manag. Sci.*, 58, 70–84 (2002).
6. A. I. Getchell, B. Subramanyam, Immediate and delayed mortality of *Rhyzopertha dominica* (Coleoptera: Bostrichidae) and *Sitophilus oryzae* (Coleoptera: Curculionidae) adults exposed to spinosad-treated commodities. *J. Econ. Entomol.*, 101, 1022–7 (2008).
7. JD. Jr. López, M. A. Latheef, B. F. Fritz, Effect of spinosad mixed with sucrose on gustatory response and mortality of adult Boll Weevils (Coleoptera: Curculionidae) by feeding and field assessment. *J. Cotton Sci.*, 16, 152–159 (2012)
8. V. L. Salgado, the modes of action of spinosad and other insect control products. *Down to Earth*, 52, 35–43 (1997).
9. G. D. Thompson, R. Dutton, T. C. Sparks, Spinosad - A case study: An example from a natural products discovery programme. *Pest Management Sci.*, 56, 696–702 (2000).
10. G. B. Watson, Actions of Insecticidal Spinosyns on  $\gamma$ -Aminobutyric Acid Responses from Small-Diameter Cockroach Neurons. *Pestic. Biochem. Physiol.*, 71, 20–28 (2001).
11. N. Orr, A. J. Shaffner, K. Richey, G. D. Crouse, Novel mode of action of spinosad: Receptor binding studies demonstrating lack of interaction with known insecticidal target sites. *Pestic. Biochem. Physiol.*, 95, 1–5 (2009).
12. G. W. Felton, C. B. Summers, Antioxidant systems in insects. *Arch. Insect Biochem. Physiol.*, 29, 187–197 (1995).
13. E. Büyükgüzel, Evidence of oxidative and antioxidative responses by *Galleria mellonella* larvae to malathion. *J. Econ. Entomol.*, 102, 152–159 (2009).
14. S. Ahmad, M. A. Beilstein, R. S. Pardini, Glutathione Peroxidase Activity in Insects : A Reassessment. *Arch. Insect Biochem. Physiol.*, 49, 31–49 (1989).
15. S. Ahmad, D. L. Duval, L. C. Weinhold, R. S. Pardini, Cabbage looper antioxidant enzymes: Tissue specificity. *Insect Biochem.*, 21, 563–572 (1991).

16. A. A. Enayati, H. Ranson, J. Hemingway, Insect glutathione transferases and insecticide resistance. *Insect Mol. Biol.*, 14, 3–8 (2005).
17. W. S. Abbott, A method of computing effectiveness of an insecticide. *J. Econ. Entomol.*, 18, 265–267 (1925).
18. M. J. Green, H. A. O. Hill, Chemistry of dioxygen. *Methods Enzymol.*, 105, 3–22 (1984).
19. H. Aebi, Catalase in vitro. *Methods Enzymol.*, 105, 121–126 (1984).
20. W. H. Habig, M. J. Pabst, W. B. Jakoby, Glutathione S transferases. The first enzymatic step in mercapturic acid formation. *J. Biol. Chem.*, 249, 7130–7139 (1974).
21. A. M. Alzahrani, S. A. Abdelsalam, O. M. Elmenshawy, A. M. Abdel-Moneim, Ultrastructural Characteristics of Spermiogenesis in *Rhynchophorus ferrugineus* (Coleoptera: Curculionidae). *Florida Entomol.*, 96, 1463–1469 (2013).
22. F. Paoli, R. Dallai,; M. Cristofaro, S. Arnone, V. Francardi, P. F. Roversi, Morphology of the male reproductive system, sperm ultrastructure and  $\gamma$ -irradiation of the red palm weevil *Rhynchophorus ferrugineus* Oliv. (Coleoptera: Dryophthoridae). *Tissue Cell*, 46, 274–285 (2014).
23. K. Hamadah, M. Tanani, Laboratory studies to compare the toxicity for three insecticides in the red palm weevil *Rhynchophorus ferrugineus*. *Int. J. Biol. Pharm. Allied Sci.*, 2, 506–519 (2013).
24. M. H. Belal, E. S. Swelam, M. A. Mohamed, Evaluation of eight insecticides belonging to four different groups for control of red palm weevil, *Rhynchophorus ferrugineus* (Olivier) (Coleoptera: Curculionidae). *Annals Agric. Sci. Moshtohor*, 50, 235–242 (2012).
25. US EPA - Spinosad pesticide fact sheet HJ 501C. EPA, Office of pesticide and toxic substances. Available online: <http://www.epa.gov/opprd001/factsheets/spinosad.pdf> (accessed on 7 April 2016).
26. N. Krishnan, D. Kodrik, Antioxidant enzymes in *Spodoptera littoralis* (Boisduval): Are they enhanced to protect gut tissues during oxidative stress? *J. Insect Physiol.*, 52, 11–20 (2006).
27. H. Al-Ayedh, M. Rizwan-ul-Haq, A. Husaain, A. Aljabr Insecticidal potency of RNAi based catalase knockdown in *Rhynchophorus ferrugineus* (Olivier) (Coleoptera: Curculionidae). *Pest. Manag. Sci.* (2016), doi: 10.1002/ps.4242.
28. A. Kolawole, A. Kolawole, Insecticides and Bio-insecticides modulate the Glutathione-related Antioxidant Defense System of Cowpea Storage Bruchid (*Callosobruchus maculatus*). *Int. J. Insect. Sci.*, 6, 79-88 (. 2014).
29. S. A. Abdelsalam, A. M. Korayem, E. A. M. Elsherbini, A. A. Abdel-Aal,; D. S. Mohamed, Photosensitizing Effects of Hematoporphyrin Dihydrochloride against the Flesh Fly *Parasarcophaga argyrostoma* (Diptera: Sarcophagidae). *Florida Entomol.*, 97, 1662-1670 (2014).
30. W. Wang, J. Mo, J. Cheng, P. Zhuang, Z. Tang, Selection and characterization of spinosad resistance in *Spodoptera exigua* (Hübner) (Lepidoptera: Noctuidae). *Pestic. Biochem. Physiol.*, 84, 180–187 (2006).

31. Y. J. Gong, Z.-H. Wang, B. C. Shi, Z. J. Kang; L. Zhu, G. H. Jin, S. J. Weig, Correlation between pesticide resistance and enzyme activity in the diamondback moth, *Plutella xylostella*. *J. Insect Sci.*, 135, 1-13 (2013).
32. H. A. Al-Daheri, M. A. Al-Deeb, Mortality and GST enzyme response of saw-toothed grain beetles, *Oryzaephilus surinamensis* (Coleoptera: Silvanidae) exposed to low insecticide concentrations. *J. Entomol.*, 9, 396–402 (2012).
33. T. A. Lambkin, M. J. Furlong, Application of Spinosad Increases the Susceptibility of Insecticide-Resistant *Alphitobius diaperinus* (Coleoptera: Tenebrionidae) to Pyrethroids. *J. Econ. Entomol.*, 107, 1590–1598 (2014).
34. A. Rehan, S. Freed, Selection, mechanism, cross resistance and stability of spinosad resistance in *Spodoptera litura* (Fabricius) (Lepidoptera: Noctuidae). *Crop Prot.*, 56, 10–15 (2014).
35. T. Shono, J. G. Scott, Spinosad resistance in the housefly, *Musca domestica*, is due to a recessive factor on autosome 1. *Pestic. Biochem. Physiol.*, 75, 1–7 (2003).
36. S. O. Abarikwu, Q. C. Duru, O. V. Chinonso, R. C. Njoku, Antioxidant enzymes activity, lipid peroxidation, oxidative damage in the testis and epididymis, and steroidogenesis in rats after co-exposure to atrazine and ethanol. *Andrologia*. 48, 548-57 (2016).
37. G. E. Abouelghar, H. Sakr, H. A. Ammar, A. Yousef, M. Nassar, Sublethal Effects of Spinosad (Tracer®) on the Cotton Leafworm (Lepidoptera: Noctuidae). *J. Plant Prot. Res.*, 53, 275–284 (2013).
38. E. Quesada-Moraga, J. A. Carrasco-Díaz, C. Santiago-Álvarez, Insecticidal and antifeedant activities of proteins secreted by entomopathogenic fungi against *Spodoptera littoralis* (Lep., Noctuidae). *J. Appl. Entomol.*, 130, 442–452 (2006).
39. K. E. Stebbins, D. M. Bond, M. N. Novilla, M. J. Reasor, Spinosad insecticide: Subchronic and chronic toxicity and lack of carcinogenicity in CD-1 mice. *Toxicol. Sci.*, 65, 276–287 (2002).
40. M. J. O'Donnell, J. P. Ianowski, S. M. Linton, M. R. Rheault, Inorganic and organic anion transport by insect renal epithelia. *Biochimica et Biophysica Acta - Biomembranes*; 1618, 194–206 (2003).
41. S. W. Nicolson, Diuresis or clearance: is there a physiological role for the 'diuretic hormone' of the desert beetle *Onymacris*? *J. Insect Physiol.*, 37, 447–452 (1991).
42. H. D. Hoyle, F. R. Turner, E. C. Raff, Axoneme-dependent tubulin modifications in singlet microtubules of the *Drosophila* sperm tail. *Cell Motil. Cytoskeleton*, 65, 295–313 (2008).
43. P. Stehrer-Schmid, H.U. Wolf, Effects of benzofuran and seven benzofuran derivatives including four carbamate insecticides in the *in vitro* porcine brain tubulin assembly assay and description of a new approach for the evaluation of the test data. *Mutat. Res.*, 339, 61–72 (1995).
44. S. Ling, R. Zhang, Effect of fipronil on brain and muscle ultrastructure of *Nilaparvata lugens* (Statl) (Homoptera: Delphacidae). *Ecotoxicol. Environ. Saf.*, 74, 1348–1354 (2011).
45. N. F. Cheville, *Ultrastructural Pathology the Comparative Cellular Basis of Disease*, Wiley-Blackwell, Second Edition (2009).

46. S. Saito, T. Yoshioka, K. Umeda, Ultrastructural effects of pyridalyl, an insecticidal agent, on epidermal cells of *Spodoptera litura* larvae and cultured insect cells Sf9. J. Pestic. Sci., 31, 335–338 (2006).

## التأثيرات البيوكيميائية والنسجية المرضية للاسباينوساد على ذكور سوسة النخيل الحمراء رانكوفوراس فيروجينيوس (أوليفر) (كوليوبترا: درايوفثريدي)

صلاح الدين عبد الرؤف عبد العزيز عبد السلام

قسم علم الحيوان والحشرات، كلية العلوم، جامعة أسيوط، مصر

سوسة النخيل الحمراء، هي مصدر قلق كبير في جميع أنحاء العالم، وخاصة في منطقة الشرق الأوسط، حيث تعتبر التمر محصول استراتيجي. وعلى الرغم من المخاطر البيئية، تبقى المبيدات الحشرية أكثر الوسائل فعالية لمكافحة الاسباينوساد، مبيد حشري بكتيري المنشأ فعال ضد العديد من الآفات، وفي هذه الدراسة جرى تقييم فعاليته ضد ذكور سوسة النخيل الحمراء. تم تحقيق استجابات لمضادات الأكسدة من الإنزيمات الرئيسية، الكاتاليز وسوبراكسيد ديسميوتيز وجلوتاسيون اس ترانسفيريز ضد عمل الاسباينوساد في المعى المتوسط والخصيتين وتم ايضا تحديد تأثيرات هذا المبيد على التركيب الدقيق لخلايا المعى المتوسط وأنابيب ملبجي والخصيتين. تم قياس التركيز القاتل لنسبة ٥٠% عند ٥٨.٨ جزء في المليون وقد ثبت المبيد انزيمات الكاتاليز وسوبراكسيد ديسميوتيز وجلوتاسيون اس ترانسفيريز في المعى المتوسط. ومع ذلك، لم يلاحظ أي تغييرات معنوية في أنشطة هذه الانزيمات في الخصيتين. المعاملة بالاسباينوساد نتج عنها تغيرات في العضيات الخلوية لخلايا المعى المتوسط وأنابيب ملبجي والخصيتين وكانت شدة هذه التغيرات معتمدة على تركيز المبيد. وبعض هذه التغيرات كانت مشابهة لتلك التي تظهرها المعاملة بالملوثات المختلفة. ومع ذلك، لوحظت تغييرات نوعيه نتيجة للمعاملة بالاسباينوساد متضمنة زيادة في اعداد واحجام المتحجرات داخل خلايا انابيب ملبجي وأحيانا فقد الزوج المركزي من الأنابيب الدقيقة من الخيوط المحورية لذبول الحيوانات المنوية. هذه الدراسة تقدم الاسباينوساد للاستخدام المحتمل كمبيد في إطار برنامج مكافحة متكامل لذكور سوسة النخيل الحمراء. بالإضافة إلى ذلك، توفر الدراسة أدلة كيميائية حيوية وتركيبية لاستخدامها في تطوير مؤشرات بيولوجية.